JMEPEG (2018) 27:4382–4391
https://doi.org/10.1007/s11665-018-3552-y

1059-9495/$19.00

Effect of Deep Cryogenic Treatment on Mechanical Properties and Microstructure of the Tool Steel CR7V for Hot Stamping

Yi Liu, Jianping Lin, Junying Min, Zhijun Ma, and Binbin Wu

(Submitted March 21, 2018; in revised form June 21, 2018; published online July 31, 2018)

To solve the failure problem of hot stamping tool, the CR7V steel was deep cryogenically treated at different dwelling times with multiple tempering. The hardness, impact toughness and wear resistance of the CR7V steel were examined, and the effects of deep cryogenic treatment on the microstructure of the CR7V steel were studied by means of optical microscope, scanning electron microscope and energy-dispersive spectroscopy. The results show that deep cryogenic treatment has little effect on the hardness of the tempered CR7V steel, but improves its impact toughness and wear resistance. The improvement in mechanical properties is a result of the combination of dissolution of large carbide particles, formation of small-sized and uniformly distributed carbide particles and fine tempered martensite structure. The cryogenic treatment is optimized as follows: vacuum gas quenching, deep cryogenic treatment at − 196 °C for 6 h and triple tempering at 560 °C for 2 h, which improves the wear resistance by 68% and the impact toughness by 58% compared to the conventional heat treatment.

Keywords carbides, deep cryogenic treatment, mechanical properties, microstructure, tempered martensite

1. Introduction

Hot stamping of ultra-high-strength steel (UHSS) has wide application in automobile industry in recent years. In hot stamping, the steel sheet is firstly heated to austenite state and transferred to tools rapidly, after which it is formed and quenched simultaneously in the tools. During this process, the contact interface of the tool, especially the fillet, is subjected to cyclic thermal and mechanical stresses, resulting in the wear failure of the tool. The wear deteriorates the shape and geometrical accuracy of the parts; on the other hand, the tool life is drastically shortened, followed by the raise of the cost and the drop of the efficiency. Therefore, it is essential to seek a feasible method to improve the mechanical properties of the tool.

Deep cryogenic treatment is a traditional process by holding the material at a low temperature below − 130 °C, generally using liquid nitrogen as a cooling medium (Ref 1). In the literature it is shown that deep cryogenic treatment can improve the mechanical properties and microstructure of the steel and extend the life of the parts. Gill et al. (Ref 2) experimented on the microstructure, hardness, wear rate and worn surface of the AISI M2 high-speed steel and concluded that the improvement in wear rate by sub-zero treatment at a temperature of − 196 °C was significantly higher than that achieved by sub-zero treatment at − 110 °C. The toughness of Vanadis 6 tool steel was proved to be improved after sub-zero treatment following high-temperature tempering (Ref 3, 4). However, when tempered at a low temperature after sub-zero treatment, the toughness of AISI D2 steel deteriorated (Ref 5). Li et al. (Ref 6) found that with the extension of the dwelling time and the increase in the repeat times, the impact toughness and wear resistance of high-vanadium alloy steel improved, but the hardness decreased. Suchmann et al. (Ref 7) found that cryogenic treatment had no effect on the strength and impact toughness of the H11 steel, but significantly increased its wear resistance at elevated temperatures. Das et al. (Ref 8) investigated the effect of various dwelling times (0-132 h) on the wear characteristics, hardness and microstructure of D2 tool steel and obtained the best parameter of cryogenic treating for 32 h by analyzing the microstructure, hardness, as well as the morphology and debris after the wear tests. There are various viewpoints on the mechanism of cryogenic treatment, among which the most widely accepted view is the transformation of retained austenite and the formation of small carbides (Ref 9-13); in addition, the cryogenic treatment alters the precipitation behavior of fine carbides (Ref 14-16). Cryogenic treatment is mainly applied to cold-working tool steels and hot forging tool steels, but rarely applied to hot stamping tool steels. In addition, cryogenic treatment parameters as well as the mechanisms are different from material to material.

The productivity is restricted by the performance of hot stamping tools in industry. Therefore, the hot stamping tool steel CR7V is cryogenically treated by different dwelling times with multiple tempering, and the effects of cryogenic parameters on the hardness, impact toughness and wear resistance of the CR7V steel are studied in this work. The mechanism is analyzed and discussed from the aspect of microstructural evolution. Optimum parameters for the heat treatment process of CR7V steel is provided, which can be a favorable reference for application.

Yi Liu, Jianping Lin, Junying Min, and **Binbin Wu**, School of Mechanical Engineering, Tongji University, Shanghai 201804, China; and **Zhijun Ma**, Shanghai Superior Die Technology Co., Ltd, Shanghai 201209, China. Contact e-mails: jplin58@tongji.edu.cn and junying.min@tongji.edu.cn.

2. Experimental Materials and Methods

The investigated tool steel is the annealed CR7V steel, and its chemical composition is listed in Table 1.

Figure 1(a) shows the conventional heat treatment process of the CR7V steel. The annealed CR7V steel was successively preheated to 650 and 850 °C, and the dwelling time was 1 h at each temperature; afterward, the material was soaked at 1030 °C for 0.5 h, and then it was quenched by vacuum gas to room temperature, followed by triple tempering at 560 °C for 2 h.

The parameters play an important role in the effect of cryogenic treatment. Most reports in the literature focus on the effects of temperature and dwelling time on the cryogenic treatment, the sequence of cryogenic treatment and tempering, repeat times and temperature of tempering, etc., among which the dwelling time of cryogenic treatment and the numbers of tempering have distinct impacts on the mechanical properties of

Table 1 Chemical composition of the CR7V steel (wt.%)

C	Si	Mn	Cr	Mo	V	P	S	Fe
0.40	0.43	0.45	6.11	1.24	0.72	0.0150	0.0010	Bal.

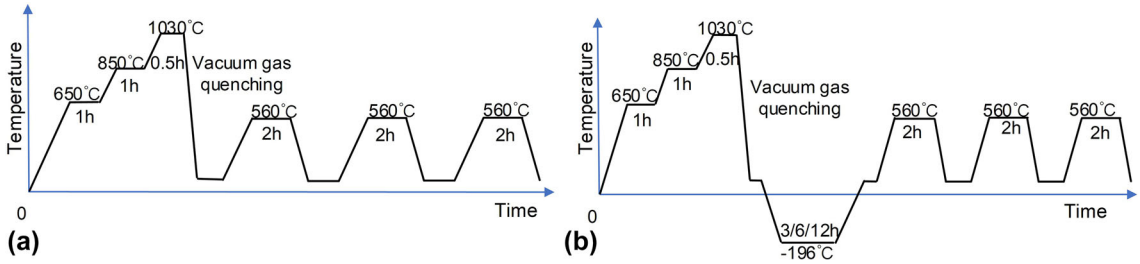

Fig. 1 Heat treatment processes of the CR7V steel: (a) conventional heat treatment and (b) deep cryogenic treatment

Table 2 Heat treatment parameters

Sample	Heat treatment procedure	
Q	Austenitization followed by air quench	…
Q + 3T		Triple tempering at 560 °C (2 h)
Q + 3C	Cryogenic treatment at − 196 °C for 3 h	…
Q + 3C + 3T		Triple tempering at 560 °C (2 h)
Q + 6C	Cryogenic treatment at − 196 °C for 6 h	…
Q + 6C + 1T		Once tempering at 560 °C (2 h)
Q + 6C + 2T		Double tempering at 560 °C (2 h)
Q + 6C + 3T		Triple tempering at 560 °C (2 h)
Q + 12C	Cryogenic treatment at − 196 °C for 12 h	…
Q + 12C + 3T		Triple tempering at 560 °C (2 h)

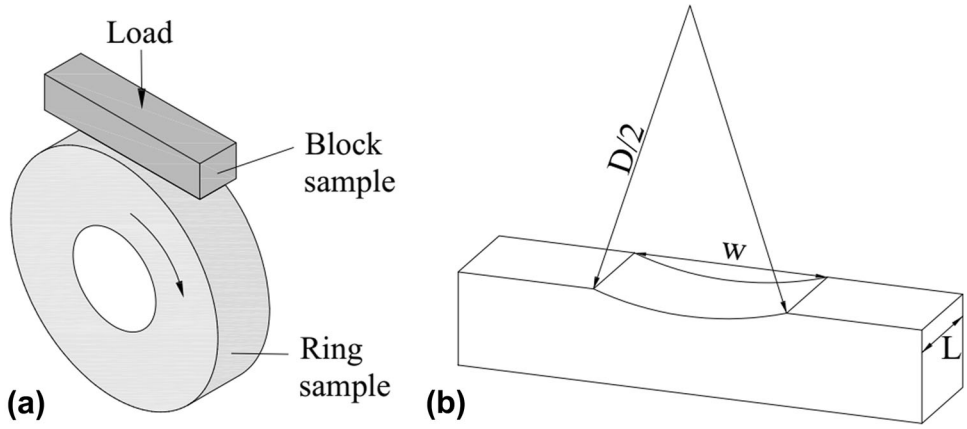

Fig. 2 Schematic of friction and wear tests: (a) contact schematic of ring/block tester; (b) schematic of wear volume

the materials (Ref 7, 10, 17). Considering their superiority and given that they are easier to control during the heat treatment process, deep cryogenic treatment processes are designed as presented in Fig. 1(b). Table 2 summarizes the parameters of the 10 investigated heat treatments.

5 mm × 5 mm × 5 mm specimens were cut out by wire electrical discharge machining, and metallographic samples were then prepared. After standard grinding and subsequent polishing procedure, the micro-hardness of each sample was measured with an HVS-1000 micro-hardness tester, and then the metallographic samples were etched with nitric acid 4%. The microstructure was observed using a DMM-300C optical microscope and an S-3400N scanning electron microscope (SEM), and the chemical elements were identified by the energy-dispersive x-ray spectroscopy (EDS). The volume fraction of retained austenite was analyzed by using an x-ray diffractometer with Cu Kα radiation at a scanning rate of 0.04°/min considering the diffraction peaks of (1 1 0), (2 0 0), (2 1 1) and (2 2 0) of martensite and (1 1 1), (2 0 0), (2 2 0) and (3 1 1) of retained austenite. Standard specimens (without any notch) having a size of 10 mm × 10 mm × 55 mm were prepared for evaluation of the fracture toughness. The impact tests were conducted at 17 °C on a JB-300B testing machine.

The wear resistance of the treated CR7V steel was tested at room temperature with a MM-2000 ring/block tester, and the tribopair is shown in Fig. 2(a). The block sample was mounted on the testing rig, while the ring rotated. The ring material was the CR7V steel with conventional heat treatment, while the block material was the CR7V steel with different cryogenic process parameters. The load was set to 50 N, the speed of the ring was 400 r/min, and the testing time was 2 h for each sample. The wear resistance of the material is evaluated normally by the mass loss and the scar width of the block sample after wear testing. Due to the influence of the external factors such as the transfer of the material and the oxide film on the specimen, an error may be introduced into the mass loss measured. Therefore, the analysis of the wear resistance based on the mass loss can be inaccurate, and the wear resistance was

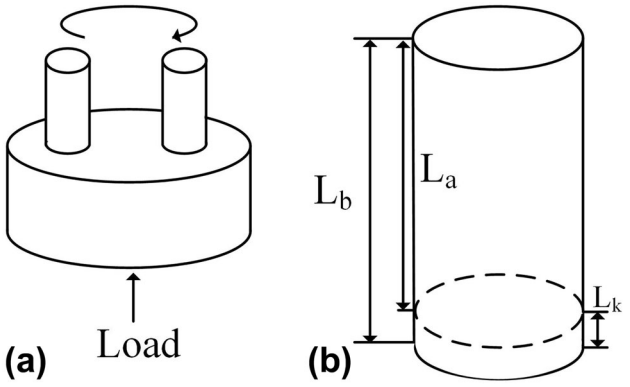

Fig. 3 Schematic of friction and wear tests: (a) contact schematic of pin-on-disk tester; (b) schematic of wear length

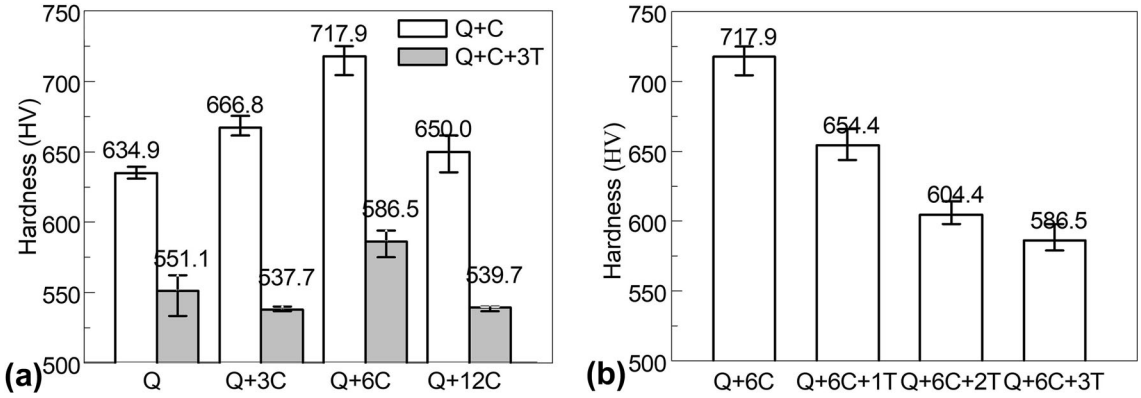

Fig. 4 Effects of (a) dwelling time in the deep cryogenic treatment and (b) multiple tempering on the hardness of the CR7V steel

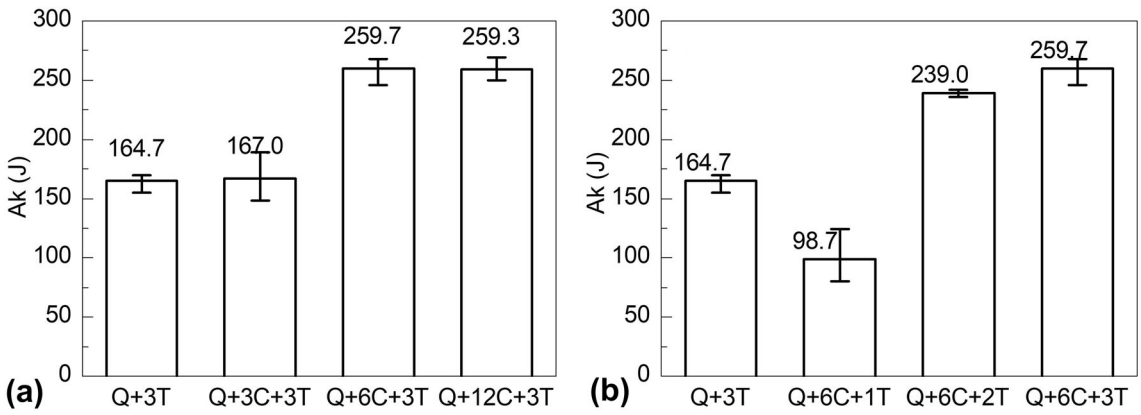

Fig. 5 Effects of (a) dwelling time in the deep cryogenic treatment and (b) multiple tempering on the impact toughness of the CR7V steel

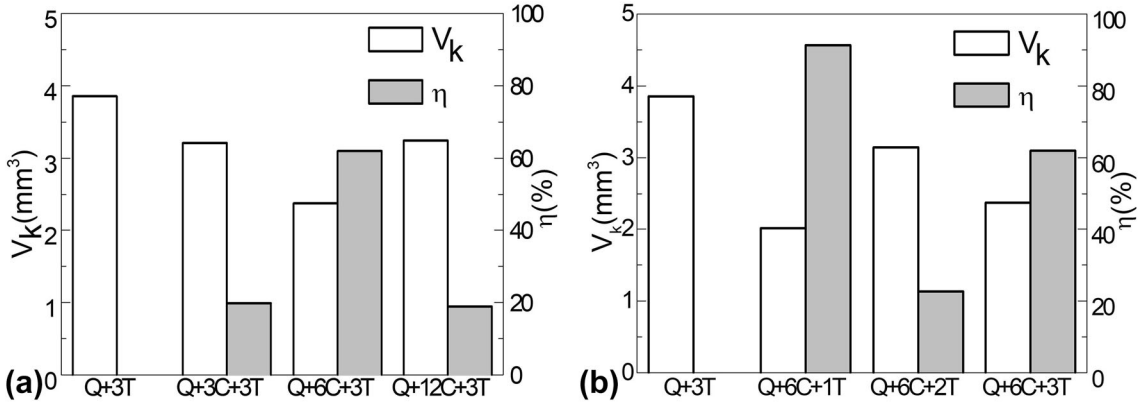

Fig. 6 Effects of (a) dwelling time in the deep cryogenic treatment and (b) multiple tempering on the wear resistance at room temperature of the CR7V steel

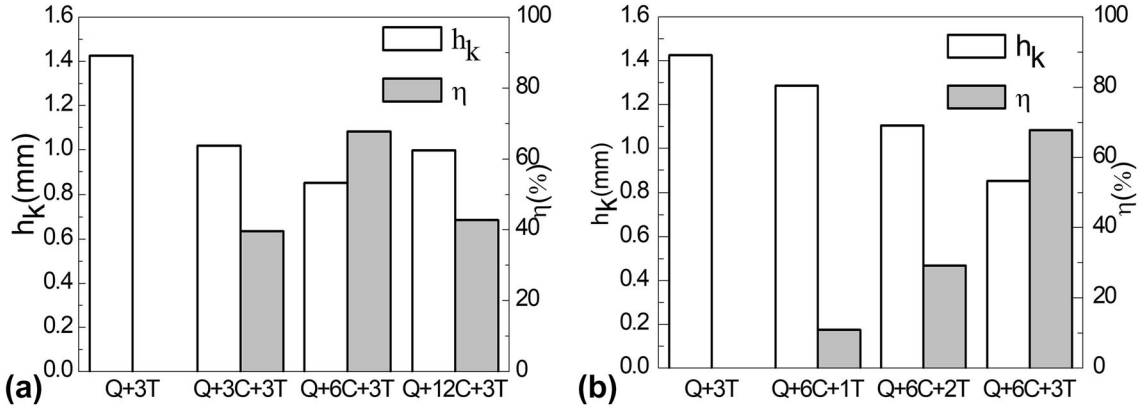

Fig. 7 Effects of (a) dwelling time in the deep cryogenic treatment and (b) multiple tempering on the wear resistance at 350 °C of the CR7V steel

then quantitatively evaluated by the wear volume calculated from the scar width. As shown in Fig. 2(b), the wear volume (V_k) can be expressed by the following formula:

$$V_k = \left(\frac{D^2}{4}\arcsin\frac{w}{D} - \frac{w}{4}\sqrt{(D^2 - w^2)}\right)L. \quad \text{(Eq 1)}$$

The relative increment of wear resistance (η) is

$$\eta = \left(\frac{V_0}{V_k} - 1\right) \times 100\%, \quad \text{(Eq 2)}$$

where D is the diameter of the ring, w is the scar width, L is the width of the block, and V_0 is the wear volume of the CR7V steel with conventional heat treatment (Q + 3T), which is regarded as a reference.

The wear resistance at elevated temperatures was tested by a pin-on-disk high-temperature friction tester, and the tribopair is shown in Fig. 3(a), where the load was set to 400 N, the rotational speed of the pin was 400 r/min, the temperature was 350 °C (according to the highest temperature of the tool reached in hot stamping), and the testing time was 1 h for each sample.

The wear resistance is evaluated by the wear length (L_k) of the pin sample [Fig. 3(b)]:

$$L_k = L_b - L_a. \quad \text{(Eq 3)}$$

The relative increment of wear resistance is as follows:

$$\eta = \left(\frac{L_0}{L_k} - 1\right) \times 100\%, \quad \text{(Eq 4)}$$

where L_k is the wear length, L_b and L_a are the length before and after the wear tests, respectively, and L_0 is the wear length of the conventional heat treatment CR7V steel, which is regarded as a reference.

3. Results and Discussion

3.1 Effect of Deep Cryogenic Treatment on the Mechanical Properties of the CR7V Steel

The effect of deep cryogenic treatment on the hardness of the CR7V steel is shown in Fig. 4. As shown in Fig. 4(a), the white bars represent the quenched samples with different cryogenic dwelling times and the shaded bars represent samples after cryogenic treatment and triple tempering process. The hardness of quenched CR7V steels increases after cryogenic

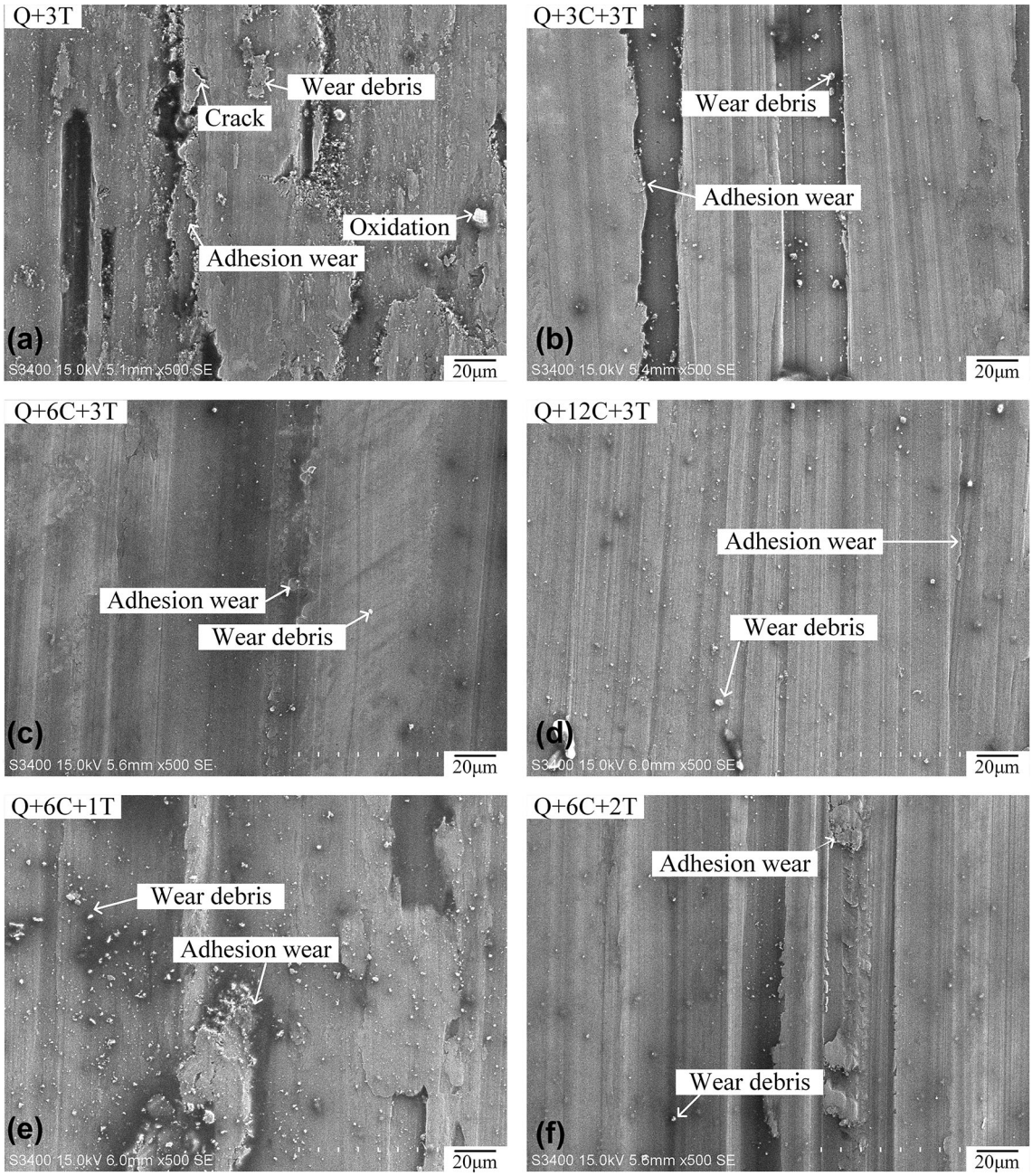

Fig. 8 Worn surfaces of different heat-treated samples: (a) Q + 3T; (b) Q + 3C + 3T; (c) Q + 6C + 3T; (d) Q + 12C + 3T; (e) Q + 6C + 1T; (f) Q + 6C + 2T

treatment, while it decreases as the dwelling time is prolonged to more than 6 h. As a result, the hardness of the specimen Q + 6C peaks at 717.9 HV. The influence of dwelling time on the hardness of tempered CR7V steel is not obvious. The hardness of specimen Q + 6C + 3T increases by 35.4 HV compared to the specimen Q + 3T, while the hardness of specimens Q + 3C + 3T and Q + 12C + 3T is basically unchanged. The effect of multiple tempering on the hardness of the CR7V steel is studied based on the specimen Q + 6C [Fig. 4(b)]. Each tempering decreases the hardness of the specimen Q + 6C, and the decreasing rate is reduced with increasing the applied tempering cycle, e.g., the decreases in the hardness are 63.5 HV, 50.0 HV and 17.9 HV after the first, second and third tempering, respectively.

The result of impact toughness of the tempered CR7V steel is provided in Fig. 5. The impact toughness varies little after cryogenic treatment for 3 h. While the impact toughness of specimens Q + 6C + 3T and Q + 12C + 3T is improved by nearly 60%, the impact toughness of the specimen Q + 6C + 3T is nearly equal to that of the specimen Q + 12C + 3T, indicating that dwelling time longer than 6 h in deep cryogenic treatment has little influence on the impact toughness of the CR7V steel. As shown in Fig. 5(b), the impact toughness of specimen Q + 6C + 1T decreases sharply compared to samples with conventional heat treatment, as a result of temper embrittlement. Temper embrittlement is mainly due to the segregation of alloying elements and impurity elements across the original austenite grain boundaries (Ref 18). In addition,

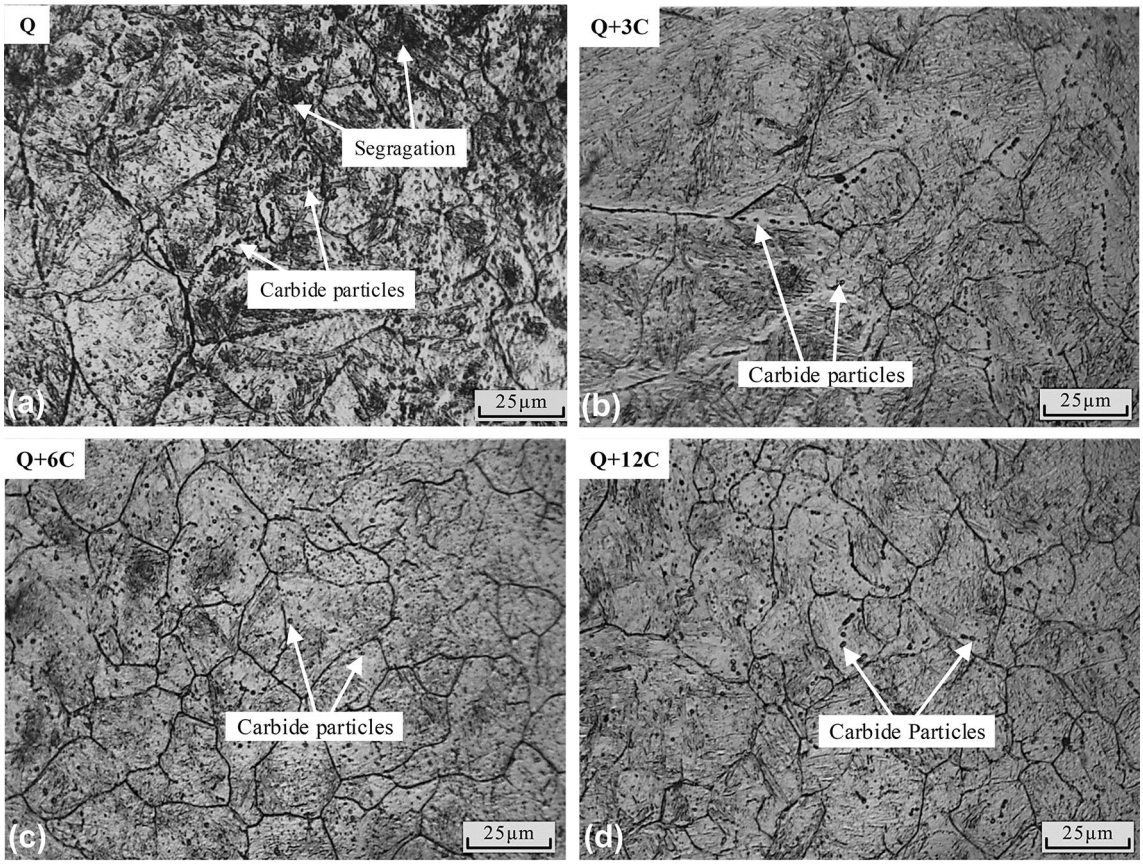

Fig. 9 Microstructure of quenching and cryogenic samples: (a) Q; (b) Q + 3C; (c) Q + 6C; (d) Q + 12C

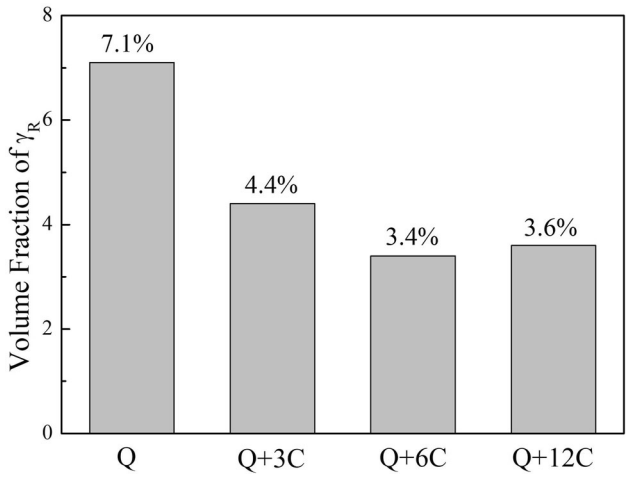

Fig. 10 Effect of dwelling time on the volume fraction of retained austenite of quenched CR7V

inadequate tempering leads to a large internal stress in the matrix, which induces brittleness. After twice tempering, the temper brittleness is eliminated and the impact toughness increases significantly by 74.3 J (45.1%) compared to the conventionally heat-treated samples. The impact toughness increases further to 259.7 J after the third tempering.

The results of wear testing at room temperature are shown in Fig. 6. The white bars are the wear volume of the wear test, and the shaded bars represent the improvement in wear resistance in contrast to conventional treatment samples. With the prolongation of the dwelling time, the wear resistance increases firstly and then decreases. The wear resistance of specimen Q + 3C + 3T is quite similar to that of the specimen Q + 12C + 3T. Cryogenic treatment for 6 h significantly increases the wear resistance by 61.98%. The wear resistance increases after cryogenic treatment for 6 h followed by multiple tempering. One cycle and three cycles of tempering have great improvements (over 60%) on the wear resistance, while the wear resistance after two cycles of tempering is increased only by 22.72%.

The results of friction and wear tests at 350 °C are presented in Fig. 7. The white bars depict the wear height of samples with different heat treatment processes, and the shaded bars indicate the improvement in wear resistance in comparison with the conventional heat treatment samples. The wear resistance of Q + 3C + 3T, Q + 6C + 3T and Q + 12C + 3T is promoted by 40, 68 and 43%, respectively. In contrast to Fig. 6, the effect of dwelling time on the wear resistance of the CR7V steel at 350 °C is similar to that at room temperature, but the effect of multiple tempering is quite different. The wear resistance at 350 °C increases with the augmentation of tempering cycles. According to the experiments on the hardness, impact toughness and wear resistance, a preferable parameter of Q + 6C + 3T is suggested.

Figure 8 typically shows the SEM images of worn surfaces for different cryogenically treated samples. Worn surfaces of cryogenic treatment samples [Fig. 8(b)-(f)] appear smoother than that of specimen Q + 3T [Fig. 8(a)]. The wear mechanism of specimen Q + 3T is a combination of adhesive wear,

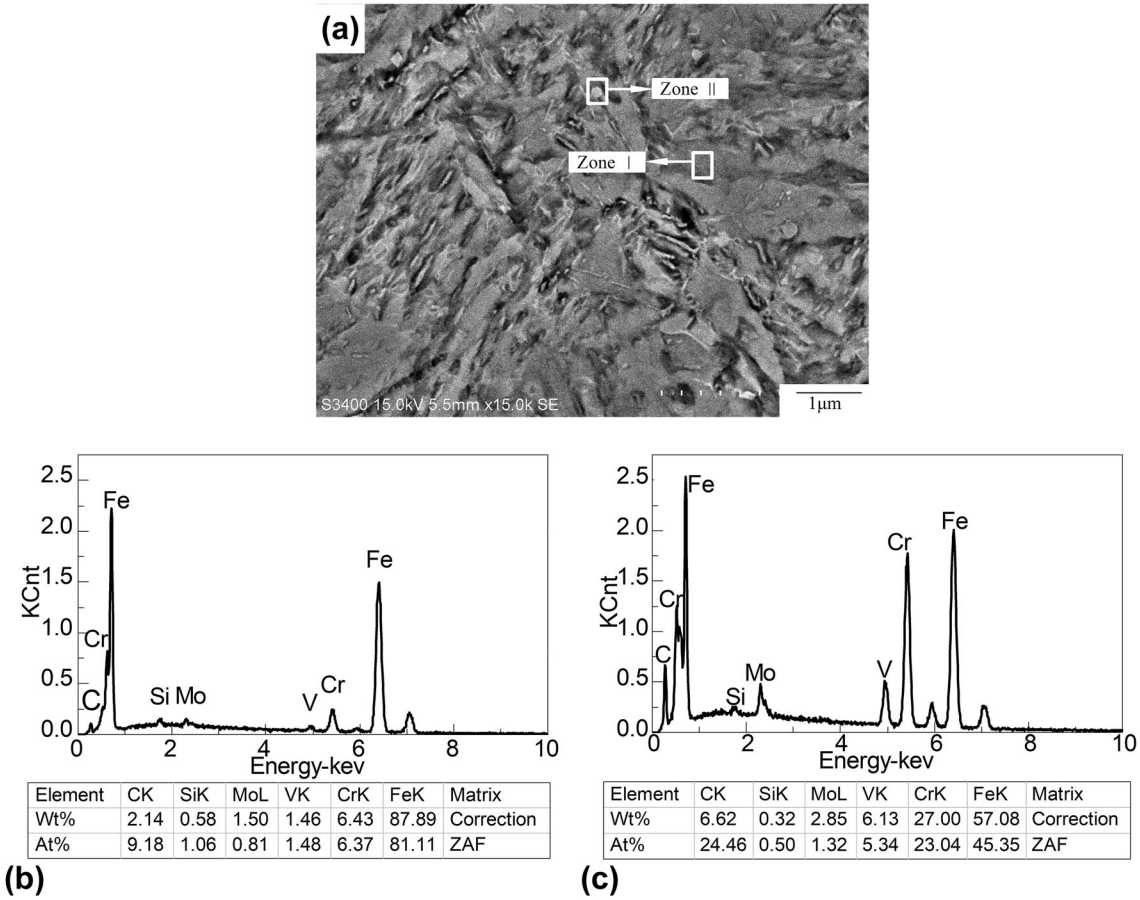

Element	CK	SiK	MoL	VK	CrK	FeK	Matrix
Wt%	2.14	0.58	1.50	1.46	6.43	87.89	Correction
At%	9.18	1.06	0.81	1.48	6.37	81.11	ZAF

Element	CK	SiK	MoL	VK	CrK	FeK	Matrix
Wt%	6.62	0.32	2.85	6.13	27.00	57.08	Correction
At%	24.46	0.50	1.32	5.34	23.04	45.35	ZAF

Fig. 11 EDS results: (a) SEM micrographs of Q + 6C + 3T; (b) EDS spectrum of Zone I; (c) EDS spectrum of Zone II

abrasive wear and oxidation wear; a crack can be observed in the image, which exacerbates the striping from the matrix. After cryogenic treatment, the wear mechanism is composed of adhesive wear and abrasive wear; furthermore, wear debris of cryogenic treatment samples is much smaller than that of Q + 3T. This observation is consistent with the wear test results, the worn surface of specimen Q + 6C + 3T is flat and just a few wear debris can be observed, and the wear mechanism is slight adhesive wear. Wear mechanism of specimens Q + 3C + 3T, 12C + 3T, Q + 6C + 2T is similar, whereas severe abrasive wear and adhesive wear happen on specimen Q + 6C + 1T.

3.2 Microstructural Evolution

Figure 9 shows the microstructures of quenched and cryogenically treated samples. Both are composed of needle-shaped martensite and carbide particles. The microstructure of specimen Q is not uniform, and the inhomogeneity is due to the segregation of alloying elements and carbides; therefore, the mechanical properties are inhomogeneous and weak. The aggregation of carbides also enhances the brittleness. Partial carbides in the specimens Q and Q + 3C are distributed in chain configuration along the grain boundaries, which are the favorable sites for the generation and extension of cracks, exacerbating the toughness (Ref 19). The chainlike carbides also deteriorate the long-term performance of the tool steel at elevated temperatures (Ref 20), which is not conducive to the application of the hot stamping tool. After cryogenic treatment for 6 and 12 h, the segregation of alloying elements and carbides was significantly reduced, and more uniform carbide particles can be observed in Fig. 9(c) and 8(d). The CR7V steel has homogeneous properties due to the relief of the segregation and the fine carbide particles, playing an important role in the improvement in the strength, hardness and wear resistance of the material.

Figure 10 depicts the evolution of retained austenite with the increase in cryogenic dwelling time. The volume fraction of γ_R can be reduced by means of deep cryogenic treatment. However, γ_R does not fully transform to martensite with the deep cryogenic treatment, and the dwelling time has little effect on the volume fraction of γ_R; furthermore, the tempering process reduces the retained austenite content obviously. Therefore, the improvement in mechanical properties of tempered CR7V is not attributed to the reduction of retained austenite.

In order to recognize the microstructural evolution during cryogenic treatment and tempering, typical SEM images are given under dry condition. As presented in Fig. 11(a), particles in the matrix were analyzed by EDS. Figure 11(b) and (c) shows the EDS spectrums of the Zone I and Zone II, respectively. It can be found that the contents of Cr, V and C of the particle increase obviously compared with the matrix; thus, the particles in the matrix can be concluded as alloy carbides. The types of carbides in the CR7V steel mainly consist of Cr, Mo and V, and the major alloy element is Cr. Cr carbide particles are more likely to grow up and become coarse

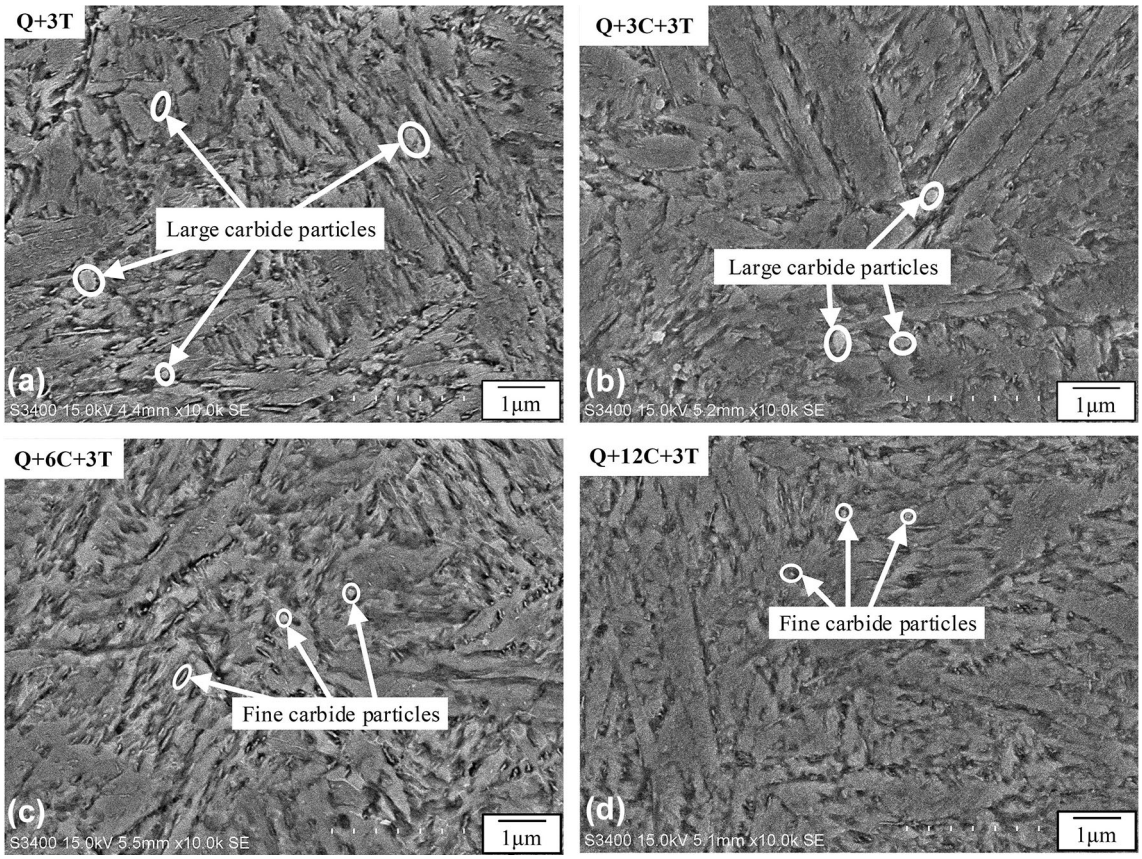

Fig. 12 SEM images of quenching and cryogenic samples: (a) Q + 3T; (b) Q + 3C + 3T; (c) Q + 6C + 3T; (d) Q + 12C + 3T

at high temperatures, forming large-sized spherical carbides (Ref 21, 22). The segregation of alloying elements and carbides are detrimental to the performance of the tool steel at elevated temperatures (Ref 23). Also, size of the carbides can be quite different; thus, the carbides are categorized as large carbide particles (size $\geq$ 0.2 μm) and fine carbide particles (size $<$ 0.2 μm).

Figure 12 presents the SEM images of specimens Q + 3T, Q + 3C + 3T, Q + 6C + 3T and Q + 12C + 3T. Large carbide particles can be observed in the sample with conventional heat treatment [Fig. 12(a)]. The carbides exhibit various shapes: The ellipsoid carbides have the length of 0.3-0.5 μm, and the dimension of the coarse acicular carbides is dissimilar, but mostly they are about 0.3-0.6 μm. There are still many coarse ellipsoidal carbides, spherical carbides and acicular carbides in specimen Q + 3C + 3T, measuring 0.3-0.5 μm [Fig. 12(b)]. With the increase in the dwelling time in the cryogenic treatment, the amount of coarse carbides is reduced significantly in the specimens Q + 6C + 3T [Fig. 12(c)] and Q + 12C + 3T [Fig. 12(d)], and the carbides are mainly granular and acicular carbide particles measuring 0.2 μm. There is also a big difference in the amount of carbides in the specimens with different dwelling times, of which the specimen Q + 6C + 3T has the largest number of carbides in comparison with the others. The fine carbides precipitated in the matrix can reduce the internal stress of the tempered martensite and reduce the sensitivity to the generation and extension of micro-cracks. The uniform distribution of precipitated carbide can also significantly enhance the toughness and wear resistance of the material. After triple tempering, the matrix is mainly composed of tempered martensite, and the specimen Q + 6C + 3T has a finer tempered martensite lattice. More refined and finer tempered martensite is beneficial to the toughness and wear resistance. The refinement of tempered martensite has been proved in Ref 4 by means of TEM, and it is considered related to the revolution of the virgin martensite (Ref 24).

Figure 13 shows the SEM images of samples cryogenically treated for 6 h followed by multiple tempering. During the tempering process, the carbides precipitated from the supersaturated α-solid solution, and the microstructures with multiple tempering are mainly needle-shaped tempered martensite and carbides after cryogenic treatment. Figure 13(b), (c) and (d) depicts typical SEM images of cryo-tempering samples, and the coarse carbides precipitated in cryogenic process become smaller and well dispersed after the tempering process compared with Fig. 13(a). Coarse spherical carbides appear in the grain after double tempering, as shown in Fig. 13(c), and the size of the carbides is about 0.3 $\sim$ 0.5 μm. The precipitation of carbides will increase the hardness of tempered martensite, but coarse carbides deteriorate the integral performance of tool steel. After once tempering [Fig. 13(b)] and triple tempering [Fig. 13(d)] no coarse carbides appear, and most of the carbides are small-sized granular carbide particles and fine acicular carbide particles. Thus, with increasing cycle numbers of tempering, the carbides in the matrix have a tendency of precipitation, coarsening and re-dissolution. There is nearly no difference in the microstructures of the specimens Q + 6C + 1T and Q + 6C + 3T, whereas the wear resistance of Q + 6C + 1T at 350 °C is worse than that of Q + 6C + 3T; accordingly, the

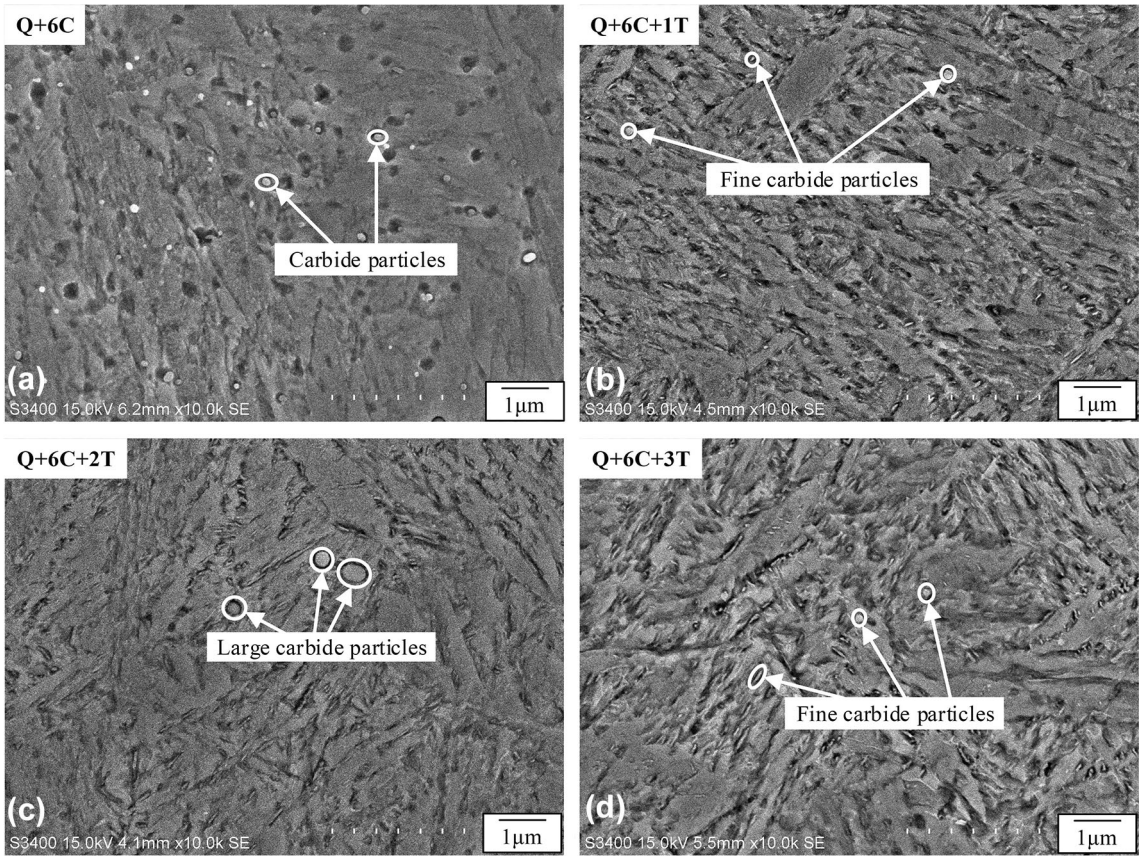

Fig. 13 SEM images of Q + 6C samples: (a) Q + 6C; (b) Q + 6C + 1T; (c) Q + 6C + 2T; (d) Q + 6C + 3T

deterioration of wear resistance of Q + 6C + 1T at elevated temperature is attributed to the decreased impact toughness.

The improvement in cryogenic treatment on the properties of CR7V steel is attributed to the combination of the shape, distribution, size of carbide particles and the morphology of tempered martensite. The fine and uniform carbides have a strengthening effect on the matrix, improving both the strength and toughness. The coarse ellipsoid, spherical carbides and coarse acicular carbides appearing in the matrix decrease the impact toughness of the material and easily act as the wear origination in high-temperature environment, reducing the wear resistance. Cryogenic treatment refines the tempered martensite, resulting in more uniform microstructures and better wear resistance.

4. Conclusions

In this study, the effects of dwelling time in the deep cryogenic treatment with multiple tempering on the hardness, impact toughness, wear resistance and microstructure of the tool steel CR7V for hot stamping were investigated, and the following conclusions can be drawn:

1. Judging from the hardness, impact toughness, wear resistance and microstructure, the optimum cryogenic parameter for hot stamping is Q + 6C + 3T, the wear resistance of which is raised by 68% and the impact toughness of which is raised by 58%.
2. The contents of retained austenite decreased after cryogenic treatment, whereas the dwelling has little influence on the transformation of retained austenite.
3. With the increase in dwelling time, small-sized granular and fine acicular carbides can be observed in the samples after cryogenic treatment for 6 and 12 h, whereas carbides in conventional heat treatment samples and samples cryogenically treated for 3 h are coarse with a shape of spherical, ellipsoid and acicular. With the increase in cycle numbers of tempering, the carbides in the matrix have a tendency of precipitation, coarsening and re-dissolution. The dispersed carbides are favorable to the improvement in impact toughness, wear resistance and other properties, and the coarse carbides decrease the impact toughness and wear resistance of the material to a certain extent.
4. After cryogenic treatment for 6 h and multiple tempering, the morphology of the tempered martensite is more refined than that of the samples after cryogenic treatment for 3 and 12 h. Fine tempered martensite helps to improve the wear resistance of the tool steel.

References

1. A. Molinari, M. Pellizzari, S. Gialanella, G. Straffelini, and K.H. Stiasny, Effect of Deep Cryogenic Treatment on the Mechanical Properties of Tool Steels, *J. Mater. Process. Technol.*, 2001, **118**(1–3), p 350–355

2. S.S. Gill, J. Singh, R. Singh, and H. Singh, Effect of Cryogenic Treatment on AISI, M2 High Speed Steel: Metallurgical and Mechanical Characterization, *J. Mater. Eng. Perform.*, 2012, **21**, p 1320–1326
3. J. Sobotova, P. Jurci, and I. Dlouhy, The Effect of Subzero Treatment on Microstructure, Fracture Toughness, and Wear Resistance of Vanadis 6 Tool Steel, *Mater. Sci. Eng. A*, 2016, **652**, p 192–204
4. J. Ptacinova, V. Sedlicka, M. Hudakova, I. Dlouhy, and P. Jurci, Microstructure—Toughness Relationships in Sub-zero Treated and Tempered Vanadis 6 Steel Compared to Conventional Treatment, *Mater. Sci. Eng. A*, 2017, **702**, p 241–258
5. D. Das, R. Sarkar, A.K. Dutta, and K.K. Ray, Influence of Sub-zero Treatment on Fracture Toughness of AISI, D2 Steel, *Mater. Sci. Eng. A*, 2010, **528**, p 589–603
6. H.Z. Li, W.P. Tong, J.J. Cui, H. Zhang, L.Q. Chen, and L. Zuo, The Influence of Deep Cryogenic Treatment on the Properties of High-Vanadium Alloy Steel, *Mater. Sci. Eng. A*, 2016, **662**, p 356–362
7. P. Suchmann, D. Jandova, and J. Niznanska, Deep Cryogenic Treatment of H11 Hot-Working Tool Steel, *Mater. Technol.*, 2015, **49**(1), p 37–42
8. D. Das, A.K. Dutta, and K.K. Ray, Optimization of the Duration of Cryogenic Processing to Maximize Wear Resistance of AISI, D2 Steel, *Cryogenics*, 2009, **49**, p 176–184
9. A. Akhbarizadeh, A. Shafyei, and M.A. Golozar, Effects of Cryogenic Treatment on Wear Behavior of D6 Tool Steel, *Mater. Des.*, 2009, **30**, p 3259–3264
10. M. Koneshlou, K.M. Asl, and F. Khomamizadeh, Effects of Cryogenic Treatment on Microstructure, Mechanical and Wear Behaviors of AISI, H13 Hot Work Tool Steel, *Cryogenics*, 2011, **51**, p 55–61
11. K. Amini, A. Akhbarizadeh, and S. Javadpour, Effect of Deep Cryogenic Treatment on the Formation of Nano-Sized Carbides and the Wear Behavior of D2 Tool Steel, *Int. J. Miner. Metall. Mater.*, 2012, **19**(9), p 795–799
12. M. Perez and F.J. Belzunce, The Effect of Deep Cryogenic Treatments on the Mechanical Properties of an AISI, H13 Steel, *Mater. Sci. Eng. A*, 2015, **624**, p 32–40
13. P. Jurči, Sub-zero Treatment of Cold Work Tool Steels—Metallurgical Background and the Effect on Microstructure and Properties, *HTM J. Heat Treat. Mater*, 2017, **72**(1), p 62–68
14. S.H. Li, L.H. Deng, and X.C. Wu, Influence of Deep Cryogenic Treatment on Microstructure and Evaluation by Internal Friction of a Tool Steel, *Cryogenics*, 2010, **50**, p 754–758
15. P. Jurči, M. Dománková, M. Hudáková, J. Ptačinová, M. Pašák, and P. Palček, Characterization of Microstructure and Tempering Response of Conventionally Quenched, Short- and Long-Time Sub-zero Treated PM Vanadis 6 Ledeburitic Tool Steel, *Mater. Charact.*, 2017, **134**, p 398–415
16. F. Meng, K. Tagashira, R. Azuma, and H. Sohma, Role of Eta-Carbide Precipitation´s in the Wear Resistance Improvements of Fe-12Cr-Mo-V-1.4C Tool Steel by Cryogenic Treatment, *ISIJ Int.*, 1994, **34**, p 205–210
17. C.H. Surberg, P. Stratton, and K. Lingenhole, The Effect of Some Heat Treatment Parameters on the Dimensional Stability of AISI, D2, *Cryogenics*, 2008, **48**, p 42–47
18. C.W. Li, L.Z. Han, G.H. Yan, Q.D. Liu, X.M. Luo, and J.F. Gu, Time-Dependent Temper Embrittlement of Reactor Pressure Vessel Steel: Correlation Between Microstructural Evolution and Mechanical Properties During Tempering at 650 °C, *J. Nucl. Mater.*, 2016, **480**, p 344–354
19. A. Cicek, F. Kara, T. Kivak, E. Ekici, and I. Uygur, Effects of Deep Cryogenic Treatment on the Wear Resistance and Mechanical Properties of AISI, H13 Hot-Work Tool Steel, *J. Mater. Eng. Perform.*, 2015, **24**, p 4431–4439
20. J. Xu, H.F. Li, C.Q. Cheng, T.S. Cao, and J. Zhao, High Temperature Performance Evaluation of As-Serviced 25Cr35Ni Type Heat-Resistant Steel Based on Stress Relaxation Tests, *J. Mater. Eng.*, 2017, **45**(8), p 96–101
21. C.H. Li, X.C. Wu, C. Xie, and H.B. Wang, Investigation on Wear Resistance of Cr8 Tool Steels, *Tribology*, 2013, **33**(1), p 35–43
22. S.H. Chen, S. Li, and X.C. Wu, High Temperature Friction and Wear Property of Hot Stamping Tool Steel SDCM, *Tribology*, 2016, **36**(5), p 538–545
23. M.X. Wei, S.Q. Wang, K.M. Chen, and X.H. Cui, Relations Between Oxidative Wear and Cr Content of Steel, *Wear*, 2011, **272**, p 110–121
24. A.I. Tyshchenko, W. Theisen, A. Oppenkowski, S. Siebert, O.N. Razumov, A.P. Skoblik, V.A. Sirosh, YuN Petrov, and V.G. Gavriljuk, Low-Temperature Martensitic Transformation and Deep Cryogenic Treatment of a Tool Steel, *Mater. Sci. Eng. A*, 2010, **527**, p 7027–7039